IEEE Photonics Journal
An IEEE Photonics Society Publication

Open Access

Ultrathin Corrugated Metallic Strips for Ultrawideband Surface Wave Trapping at Terahertz Frequencies

Volume 9, Number 1, February 2017

Yan Liu
Cizhe Fang
Genquan Han, *Member, IEEE*
Yao Shao
Yan Huang
Hongjuan Wang
Yibo Wang
Chunfu Zhang
Yue Hao, *Senior Member, IEEE*

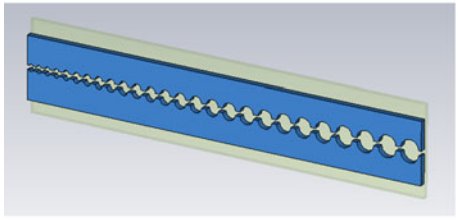

(a)

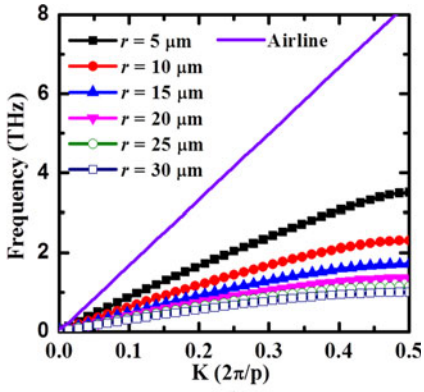

(b)

DOI: 10.1109/JPHOT.2016.2633864
1943-0655 © 2016 IEEE

IEEE photonics SOCIETY

IEEE

Ultrathin Corrugated Metallic Strips for Ultrawideband Surface Wave Trapping at Terahertz Frequencies

Yan Liu,[1] Cizhe Fang,[1] Genquan Han,[1] *Member, IEEE*, Yao Shao,[2] Yan Huang,[1] Hongjuan Wang,[1] Yibo Wang,[1] Chunfu Zhang,[1] and Yue Hao,[1] *Senior Member, IEEE*

[1]Wide Bandgap Semiconductor Technology Disciplines State Key Laboratory, School of Microelectronics, Xidian University, Xi'an 710071, China
[2]China Electric Power Research Institute, Beijing 100192, China

DOI:10.1109/JPHOT.2016.2633864

Manuscript received October 16, 2016; revised November 21, 2016; accepted November 27, 2016. Date of publication December 1, 2016; date of current version January 10, 2017. This work was supported by the National Natural Science Foundation of China under Grant 61534004, Grant 61604112, and Grant 61622405. Corresponding author: G. Han (e-mail: hangenquan@ieee.org).

Abstract: The dispersion properties of the ultrathin spoof slow-wave plasmonic waveguide based on different ultrathin metal strip grooves have been simulated using the finite element method. The dispersion characteristics of the four different surface plasmon polariton (SPP) waves are thoroughly analyzed by the dispersion curves, electric intensity distribution, and power flow distribution. As a conclusion, the gradient arch-shape waveguide has been chosen as an ideal slow-wave system for trapping SPP waves. Furthermore, the reflected location for the SPP waves on the arch-shape corrugated metal strip at different frequencies has been compared by three methods. It is demonstrated that such an ultrathin gradient arch-shape waveguide provides an ultrawideband performance for trapping surface waves, which permits broadband trapping of terahertz radiation.

Index Terms: Spoof surface plasmon polaritons (SPPs), metallic grooves

1. Introduction

Since 2001, the slow wave system, first studied in the field of atomic coherence [1], has been comprehensively analyzed due to its potential to manipulate light for both optical communication networks and quantum information processing systems. Most of these systems have been focused on photonic crystal waveguide [2], [3], electromagnetically induced transparency [4], quantum-dot semiconductor optical amplifiers [5], direct coupled resonators [6], coherent population oscillations [7], stimulated Brillouin scattering [8], stimulated Raman scattering [9], metamaterials [10], and surface plasmon polaritons (SPPs) [11]–[13]. Among above methods, SPPs, as a new and attractive approach for trapping light, has obtained much attention due to their potential for strong confinement of electromagnetic wave in the subwavelength scale over broadband. However, in the terahertz (THz) frequency range, there are only a few pioneers focusing on this issue, such as Gan qiao qiang *et al* at Lehigh University [11]. It is generally known that metal behaves like a perfect electric conductor (PEC) and can not support SPPs in the THz frequencies [14], so certain surface structures were designed termed "spoof SPPs" to overcome this limitation [15]. Furthermore, various surface structures, such as graded metallic grating [11], [16], graphene monolayer [17], [18], corrugated wire [19],

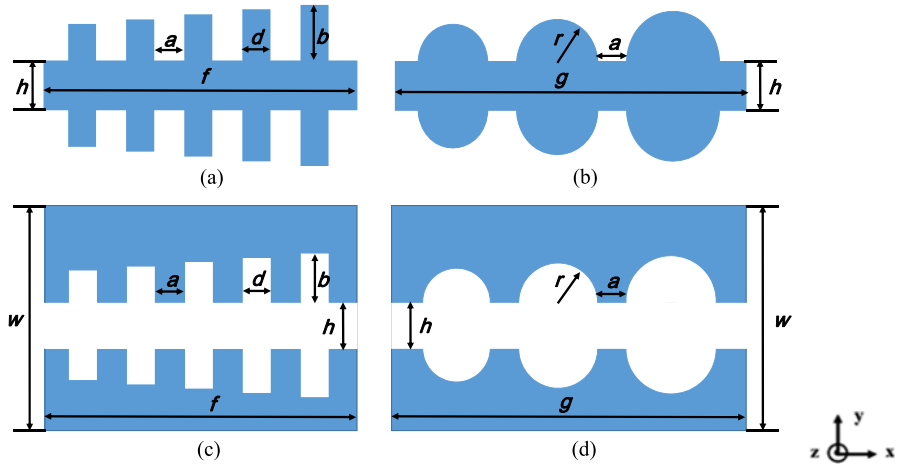

Fig. 1. Schematics of the designed spoof plasmonic waveguides with (a) double grating, (b) dumbbell-shape, (c) comb-shape, and (d) arch-shape structures.

tapered waveguide with a negative refractive index core [10], [20], and hole arrays [21] have been utilized to slow light to a certain standstill at different locations. For example, a subwavelength metal grating waveguide consisting of two parallel metal slabs with the periodic corrugations on their inner boundaries is designed to slow light at THz frequencies [22], [23]. Such structures for the purpose of spatial confinement and slow light make these THz photonic devices relative bulky. To realize miniaturization, an ultrathin corrugated metallic structure has been proposed to realize more compact plasmonic devices and circuits [24]–[31]. Based on this planar ultrathin plasmonic structure, they have designed a waveguide to trap broadband spoof SPP waves in the microwave frequency, which is also been verified by experiments [32].

In this paper, the dispersion characteristics of plasmonic metamaterials on ultrathin slow-wave plasmonic waveguides with nearly zero thickness in the terahertz frequencies are investigated. The propagation properties of the spoof SPPs on the arch-shape waveguide are comprehensively analyzed by different simulation methods. Such planar plasmonic waveguide based on a gradient arch-shape exhibits an excellent trapping capability for improving the performance of the spectrometer, filter, biosensors, and integrated high-density devices in THz bands.

2. SPP dispersion of slow-wave plasmonic waveguides

To analyze the SPPs dispersion of 3-D slow-wave plasmonic waveguides thoroughly, we first characterize the dispersion relation of the corrugated metal grooves with various structures, as shown in Fig. 1, using the CST microwave Studio. The metal is modeled as a perfect electrical conductor (PEC) in the calculations due to its highly electric conductivity in the terahertz region [14], therefore, the metal loss can be ignored. The thickness of the ultrathin metal strip is 0.1 μm. The dielectric substrate for the structures has a thickness and a relative dielectric constant of 20 μm and 2.9, respectively. The first proposed spoof plasmonic waveguide is named “double grating”, as illustrated in Fig. 1(a), which consists two metal grating strips extending along opposite direction in the *y* direction with gradient heights. The height *b* increases from 5 to 30 μm with a step of 1 μm. The width *d* and gap *a* are 5 and 16 μm, respectively. The distance *h* between two grating bottoms is set to be 15 μm. The structure in Fig. 1(c) is denoted as “comb-shape” structure, which can be regarded as a complementary structure compared with Fig. 1(a). The structure of comb-shape can be obtained by subtracting a double grating structure in Fig. 1(a) from an original metal strip, which has a length *f* of 546 μm and a *w* of 205 μm. This kind of double grating structure also consists 26 periods. For Fig. 1(b) and (d), the two structures are a pair of complementary structures in the same way, which are denoted as “dumbbell-shape” and “arch-shape” structure, respectively.

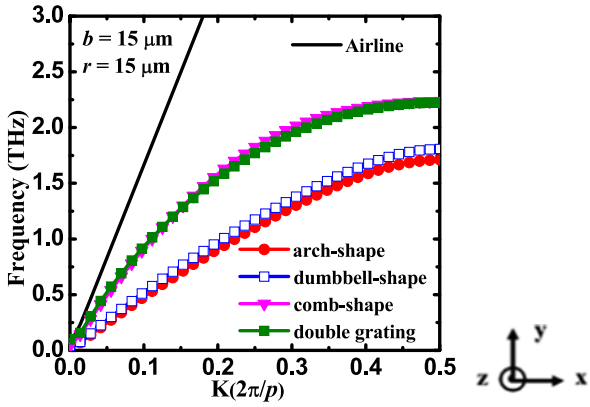

Fig. 2. Dispersion relations of SPPs in one unit of the four different structures for $b = 15\,\mu$m and $r = 15|\,\mu$m.

The dumbbell-shape structure in Fig. 1(b) is composed of a series of semi-circles with radius increasing progressively. Here the radius r of the semi-circle increases from 5 to 30 μm with a step of 1 μm, when fixing the distance between adjacent periods is 16 μm. Therefore, the whole length g of the metal strip is 1326 μm with 26 periods. The height w of the whole metal strip and the distance h between two semicircle series in Fig. 1(b) and (d) remain the same as those in Fig. 1(a) and (c).

The dispersion relations of the above four slow-wave structures calculated by an eigenmode solver of CST Microwave Studio are plotted in Fig. 2, in which four periodic unit cells for these four structures shown in Fig. 1 are located in an outer air box respectively. The outer air box has the same size as the periodic cell in the x direction and is larger than the unit cell in the y and z directions. For the air box, the boundaries in the x direction should be set as master and slave boundaries (i.e. the periodic boundary), and the boundaries in the y and z directions are set as PEC. For a given phase difference as a variable swept from 0^o to 180^o between the master and slave boundaries, we can calculate all eigenfrequencies using the Eigen-mode solver. Then, the dispersion relation can be directly output. The height b of one unit for double grating and comb-shape structure and the diameter r of one unit for dumbbell-shape and arch-shape structure are both fixed to be 15 μm. In simulation, one unit for all the four structures will infinitely repeat in the x direction, which means it still is a slow-wave system. It can be seen that the dispersion curves of SPPs on two semi-circle shapes are much lower than those in two rectangular shapes. When the same shape is considered, the two dispersion curves almost overlap with each other. At the first Brillouin zone boundary, the corresponding asymptotic frequency for the arch-shape is 1.71 THz, which is the minimum value in these four structures. Since the wave vectors of SPPs in the arch-shape are larger compared to other structures, it exhibits more deviation from the light line due to stronger confinement.

To further evaluate the dispersion characteristics of SPPs on different structures, we extract the electric field intensity distributions on the four slow-wave waveguides at 1 THz. Using CST Microwave Studio, the simulated electric field distributions are observed on a plane that is 2 μm above the metallic strip in the z direction. As b and r vary from 5 to 30 μm in a step of 1 μm, it can be seen that the electric field intensity are concentrated periodically along the whole propagation path. For these two upper structures in Fig. 3(a) and (b), the highest electric field intensity is usually localized at the upper and bottom boundary of metal strip. However, for the two lower structures in Fig. 3(c) and (d), the highest electric field intensity is localized in the middle area of the metal strip. Since the metal loss is ignored in THz region, it shows little electric field distribution in the upper and bottom area of the two lower structures in Fig. 3(c) and (d). What's more, it can be concluded that the double grating and dumbbell-shape structures have a little higher propagation loss due to light radiation in the air than those of the other two structures. Consequently, these two upper structures will result in a lower propagation efficiency and a shorter propagation length, which will be discussed in detail in the latter content. On the other hand, the high propagation efficiency for the

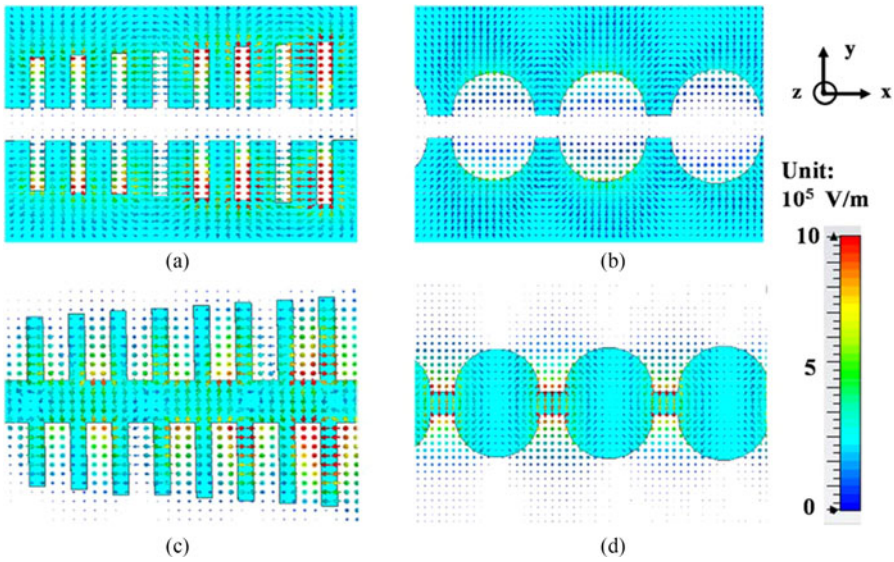

Fig. 3. Electric field intensity distributions on the four kinds of slow-wave waveguides at 1 THz with (a) double grating structure, (b) dumbbell-shape structure, (c) comb-shape structure, and (d) arch-shape structure.

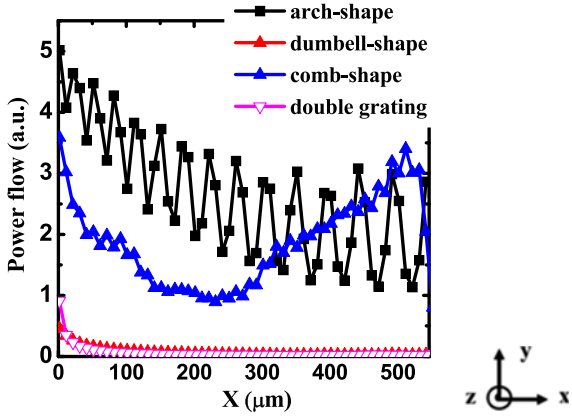

Fig. 4. Power flow distributions along the central line at 1 THz for the structures in Fig. 3.

comb-shape and arch-shape structures can also be attributed to placing two opposite metal strips together in the y direction, which will lead to less radiation loss and stronger confinement for SPPs wave due to the reflection between the two reverse placed metal strips. In a word, it comes to the conclusion that the dispersion characteristics not only depends on the dimension of the waveguide structures but also depends on the propagation path of the different waveguides.

To verify the conclusion deduced from Fig. 3, the power flow distributions for the above four structures along the central line in the middle of the *y* direction at 1 THz is analyzed in Fig. 4. In order to estimate the propagation efficiencies of the above four structures along the same propagation length, the whole length $f = 546\,\mu$m for the double grating and comb-shape structures is chosen for the whole length in the x direction. Then, the power of the face at 0 μm and the power of the face at 546 μm are defined to be P_1 and P_2, respectively. Thus, the attenuation coefficients α can be calculated by $\ln(P_1/P_2)/2f$. For the four structures in Fig. 4, it can be noticed that the attenuation coefficients α of the double grating and dumbbell-shape structures are much larger than those of the other two, which indicate much shorter propagation length. Only taking the attenuation coefficient into account, the comb-shape structure and the arch-shape structure show almost the same α at all. When the curves in Fig. 4 for these two structures are considered, the cases are a

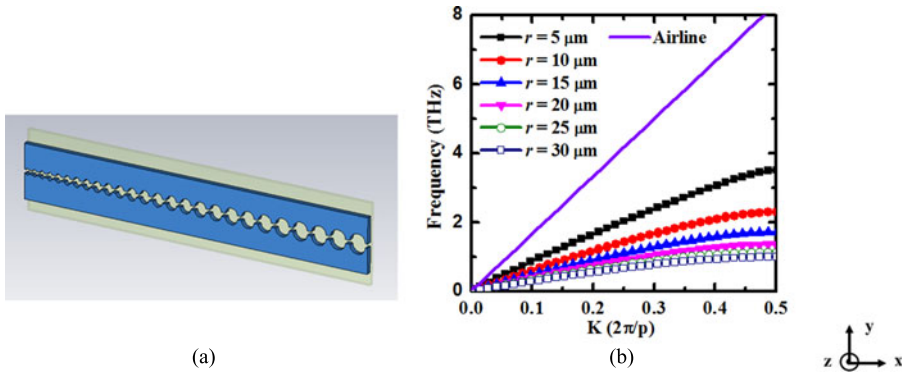

Fig. 5. (a) Three-dimensional schematic of the designed arch-shape waveguide with gradient radii. (b) Dispersion curves of one unit of the designed arch-shape waveguide with different radii varying from 5 μm to 30 μm at a step of 5 μm, in which the purple line is the airline. The other parameters are set to be the same as those in Fig. 1(d).

little complicated. Before x is 250 μm, the power along the comb-shape waveguide decays more rapidly than that along the arch-shape waveguide. However, when x is larger than 250 μm, the power along the comb-shape shows a peak near 500 μm abnormally, which appears to corroborate the electric field intensity vector in Fig. 3(c). From the electric field intensity distribution in Fig. 3(c), it exhibits that the higher electric field vectors are mostly concentrated in the middle area at the end of the comb-shape waveguide, which implies that the combined effect of much stronger SPP derived from deeper rectangular grooves at the end of the waveguide and the reflection of each other between the neighboring upper and under gratings. However, for an arch-shape waveguide, it demonstrates an electric field intensity concentration periodically varying in Fig. 3(d) and a periodic oscillatory variation in Fig. 4, which indicates the controllability for the purpose of slow-wave system. Such a difference in power flow between these two structures can be attributed to the difference of multistage diffraction ability between the shapes of rectangle and semi-circle. For the purpose of slow-wave system, the arch-shape waveguide was chosen to be the ideal structure used in the following content.

3. SPPs propagation of slow-wave plasmonic waveguide

To further investigate the propagation property of the proposed arch-shape waveguide illustrated in Fig. 5(a), the dispersion curves of SPPs on one unit of such grooves with a gradient disk radius are calculated and plotted in Fig. 5(b). In simulation, one unit for this structure also infinitely repeats in the x direction. It can be noticed that for the arch grooves, the bigger the radius of the disk is, the lower the dispersion curve is. What is more, the deviation between the dispersion curve and the airline is closely related to the confinement ability of SPP waves. When the radius is 30 μm, the asymptotic frequency is nearly 1 THz, which implies the largest mismatch between the wave vector of SPPs and that of the free-space waves and the strongest confinement of the propagating EM waves at the surface among all the grooves. On the other hand, with the radius increases, the dispersion curves almost overlap with little variations, especially for the radii of 25 μm and 30 μm. Because most of the highest electric field intensities are periodically concentrated along the gap between two disks in Fig. 3(d), it can be speculated that the reflection between the upper and under arch structures can be negligible for larger sizes. As the semi-circle's radius is larger than 25 μm, the difference in sizes has almost no influence on the confinement ability and the cutoff frequency will be a constant value. When consider a gradient arch-shape waveguide as shown in Fig. 5(a), where the radius of the aperture is graded linearly from 5 to 30 μm at a step of 1 μm, and the corresponding dispersion relations for the whole structure also vary within the frequency ranges from 1 to 3.5 THz as a function of the position along the propagation direction. Such broadband EM

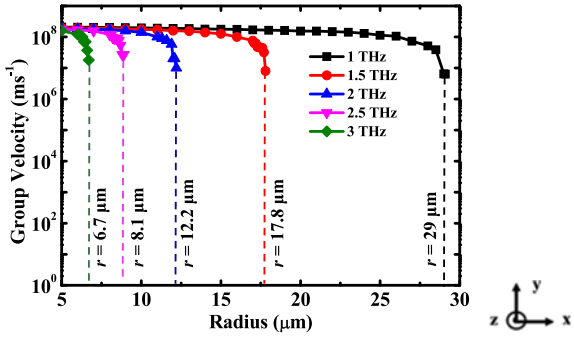

Fig. 6. Group velocity of the spoof SPPs on the designed arch-waveguide with gradient radii at different frequencies.

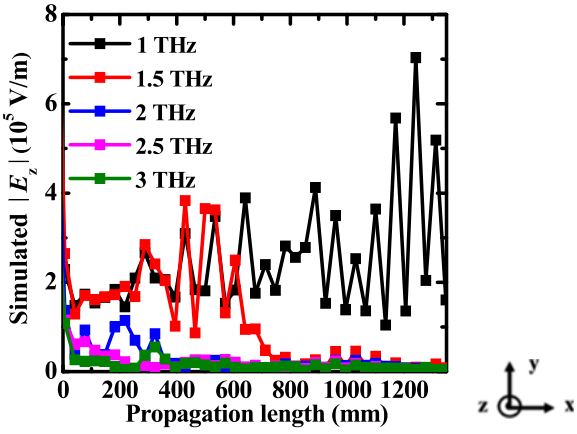

Fig. 7. Simulated electric-field vertical $|E_z|$ distributions of the arch-shape waveguide along the x direction for different frequencies.

wave can be slow down gradually in this graded arch-shape structure, showing an ultra-wideband capability of this design.

From Fig. 5(b), the group velocity can be obtained from the slope of the tangent line at different frequencies on the dispersion curve. Fig. 6 shows group velocity of the spoof SPPs on the designed ultrathin plasmonic arch-shape waveguide printed on the dielectric substrate at different frequencies. From the simulated data, the symbols with the solid lines can only describe the group velocity down to near 10^7 ms^{-1}, which is limited by the data amount. In theory, if the radius step is sufficient small, the group velocity can gradually decrease to zero with a sufficient small step, which can not be realized in this designed waveguide due to the radius step limitation. To make the slow-wave process more specific, the dashed lines down to 10^0 are added as the auxiliary lines. In principle, depending on the varying frequency, the EM waves can be regarded as "trapped" at different locations by the surface of such arch structures when the group velocity is below 10^7 ms^{-1}. As for the whole waveguide, the SPP's group velocity will decrease gradually when propagating along the corrugated strip. It is worth noting that at a specific frequency as the radius of the semi-circle increases, the group velocity decreases. For instance, the EM wave at the frequency of 1 THz is almost "trapped" at the location where the radius is 29 μm, whereas that at 3 THz is localized at the radius of 6.7 μm.

To evaluate the reflected location of SPP waves on the corrugated metal strip at different frequencies, the electric-field vertical $|E_Z|$ distributions of the arch-waveguide along the central line on the metal strip in Fig. 5(a) are simulated in Fig. 7. From the peaks of the oscillation wave in it, it can be deduced that the spoof SPPs reflect at $x = 1243$, 428, 217, 78, and 31 mm in frequencies of 1, 1.5, 2, 2.5, and 3 THz, respectively. From the results illustrated in Fig. 6, the propagation

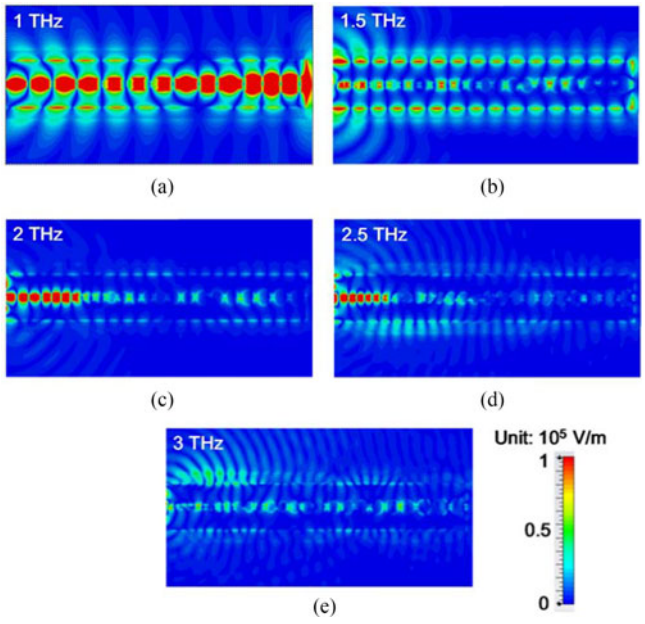

Fig. 8. Two-dimensional electric field magnitude distributions of the arch-shape waveguide at different frequencies. (a) 1 THz, (b) 1.5 THz, (c) 2 THz, (d) 2.5 THz, and (e) 3 THz.

distance corresponding to zero group velocity can also be calculated by the geometry parameters in the simulation. For the frequencies 1, 1.5, 2, 2.5, and 3 THz, the radii $r = 29$, 17.8, 12.2, 8.1, and 6.7 μm correspond to the propagation distances $x = 1250$, 494, 264, 116,and 54 mm. Hence, the difference of propagation distances between Fig. 6 and Fig. 7 can be ascribed to the radii in calculation process is rounded to the nearest radii due to a radius step of 1 μm in Fig. 6. To further verify these reflection location, a comparison analysis on the 2-D electric field magnitude distributions on an observation plane that is 2 μm above the strip in Fig. 5(a) is carried out in Fig. 8. The whole metal strip is excited by an electric monopole with unity current at the input end. In the simulation, the electric monopole consists of a PEC circular ring cylinder, a circular ring cylinder with the relative dielectric constant of 2.55 and a PEC slender cylinder in the center. From Fig. 7 and Fig. 8, it can be seen that the propagation distances for the two simulation methods are almost consistent, except that the reflected locations have a little deviation. At the same frequency, the strongest electric-field magnitude distributions corresponding to the peaks in Fig. 7 are depicted as red color in Fig. 8, showing the similar trapping ability for SPP waves. In Fig. 8(a) and (b), obvious light field leakage can be observed at the upper and lower edges of the whole metal strip, which can be attributed to the mismatch between the transverse magnetic mode in the monopole and the principal mode in the strip.

4. Conclusion

In summary, the dispersion characteristics for the spoof SPPs based on different corrugated metal groove structures are comprehensively studied using finite element method. Based on the conclusion of the comparison, the slow-wave plasmonic waveguide with arch-shape has been analyzed thoroughly and its dispersion relation and propagation characteristic have been observed. Through the calculations of group velocity, electric field absolute value distribution and electric field magnitude distribution, the propagation distances of SPPs on the gradient plasmonic waveguide are in excellent agreement, which exhibits a good trapping ability as a slow-wave system. It has been demonstrated that this gradient corrugated plasmonic waveguide can control slow light with elaborate designing, which can contribute to realizing compact plasmonic function devices at THz frequencies.

References

[1] C. Liu, Z. Dutton, C. H. Behroozi, and L. V. Hau, "Observation of coherent optical information storage in an atomic medium using halted light pulses," *Nature*, vol. 409, no. 6819, pp. 490–493, 2001.

[2] Y. A. Vlasov, M. O'Boyle, H. F. Hamann, and S. J. McNab, "Active control of slow light on a chip with photonic crystal waveguides," *Nature*, vol. 438, no. 7064, pp. 65–69, 2005.

[3] H. Gersen *et al*., "Real-space observation of ultraslow light in photonic crystal waveguides," *Phys. Rev. Lett.*, vol. 94, no. 7, 2005, Art. no. 073903.

[4] M. D. Lukin and A. Imamoglu, "Controlling photons using electromagnetically induced transparency," *Nature*, vol. 413, no. 6853, pp. 273–276, 2001.

[5] E. Gehrig, M. van der Poel, J. Mørk, and O. Hess, "Dynamic spatiotemporal speed control of ultrashort pulses in quantum-dot SOAs," *IEEE J. Quantum Electron.*, vol. 42, no. 10, pp. 1047–1054, Oct. 2006.

[6] A. Melloni, F. Morichetti, and M. Martinelli, "Optical slow wave structures," *Opt. Photon. News*, vol. 14, pp. 44–48, 2003.

[7] M. S. Bigelow, N. N. Lepeshkin, and R. W. Boyd, "Superluminal and slow light propagation in a room-temperature solid," *Science*, vol. 301, pp. 200–202, 2003.

[8] Y. Okawachi *et al*., "Tunable all-optical delays via brillouin slow light in an optical fiber," *Phys. Rev. Lett*, vol. 94, no. 15, 2005, Art. no.153902.

[9] K. Lee and N. M. Lawandy, "Optically induced pulse delay in a solid-state Raman amplifier," *Appl. Phys. Lett.* vol. 78, no. 6, pp. 703–705, 2001.

[10] K. L. Tsakmakidis, A. D. Boardman, and O. Hess, "Trapped rainbow storage of light in metamaterials," *Nature*, vol. 450, no. 7168, pp. 397–401, 2007.

[11] Q. Gan, Z. Fu, Y. Ding, and F. Bartoli, "Ultra-wideband slow light system based on THz plasmonic graded metallic grating structures," *Phys. Rev. Lett.*, vol. 100, 2008. Art. no. 256803.

[12] M. I. Stockman, "Nanofocusing of optical energy in tapered plasmonic waveguides," *Phys. Rev. Lett.*, vol. 93, no. 13, 2004. Art. no.137404.

[13] M. Sandtke and L. Kuipers, "Slow guided surface plasmons at telecom frequencies," *Nature Photon.*, vol. 1, no. 10, pp. 3081–3084, 2007.

[14] S. A. Maier, *Plasmonics: Fundamentals and Applications*. New York, NY, USA: Springer-Verlag, 2007.

[15] S. A. Maier and S. R. Andrews, "Terahertz pulse propagation using plasmon-polariton-like surface modes on structured conductive surfaces," *Appl. Phys. Lett.*, vol. 88, no. 25, 2006. Art. no. 251120.

[16] Z. Fu, Q. Gan, Y. J. Ding, and F. J. Bartoli, "From waveguiding to spatial localization of THz waves within a plasmonic metallic grating," *IEEE J. Sel. Topics Quantum Electron.*, vol. 14, no. 2, pp. 486–490, Mar./Apr. 2008.

[17] L. Chen, T. Zhang, X. Li, and G. P. Wang, "Plasmonic rainbow trapping by a grapheme monolayer on a silicon grating substrate," *Opt. Exp.*, vol. 21, no. 23, pp. 28628–28637, 2013.

[18] X. Yin, T. Zhang, L. Chen, and X. Li, "Plasmonic rainbow trapping by a silica-graphene-silica on a sloping silicon substrate," *IEEE J. Lightw. Technol.*, vol. 32, no. 21, pp. 3591–3596, Nov. 2014.

[19] S. A. Maier, S. R. Andrews, L. Martin-Moreno, and F. J. Garcia-Vidal, "Terahertz surface plasmon-polariton propagation and focusing on periodically corrugated metal wires," *Phys. Rev. Lett.*, vol. 97, no. 17, 2006, Art. no. 176805.

[20] E. I. Kirby, J. M. Hamm, K. L. Tsakmakidis, and O. Hess, "FDTD analysis of slow light propagation in negative-refractive-index metamaterial waveguides," *J. Opt. A, Pure Appl. Opt.*, vol. 11, no. 11, pp. 114027-1–114027-6, 2009.

[21] J. B. Pendry, L. Martin-Moreno, and F. J. Garcia-Vidal, "Mimicking surface plasmons with structured surfaces," *Science*, vol. 305, no. 5658, pp. 847–848, Aug. 2004.

[22] J. Zhang, L. Cai, W. Bai, Y. Xu, and G. Song, "Slow light at terahertz frequencies in surface plasmonpolariton assisted grating waveguide," *J. Appl. Phys.*, vol. 106, no. 10, 2009, Art. no. 103715.

[23] B. Wang, Y. Jin, and S. He, "Design of subwavelength corrugated metal waveguides for slow waves at terahertz frequencies," *Appl. Opt.* vol. 47, no. 21, pp. 3694–3700, 2008.

[24] X. P. Shen, T. J. Cui, D. Martin-Cano, and F. J. García-Vidal, "Conformal surface plasmons propagating on ultrathin and flexible films," *Proc. Nat. Acad. Sci.*, vol. 110, no. 1, pp. 40–45, Jan. 2013.

[25] X. Shen and T. J. Cui, "Planar plasmonic metamaterial on a thin film with nearly zero thickness," *Appl. Phys. Lett.*, vol. 102, no. 21, 2013, Art. no. 211909.

[26] X. Gao *et al*., "Ultrathin dual-band surface plasmonic polariton waveguide and frequency splitter in microwave frequencies," *Appl. Phys. Lett.*, vol. 102, no. 15, Apr. 2013, Art. no. 151912.

[27] X. Gao, L. Zhou, Z. Liao, H. F. Ma, and T. J. Cui, "An ultra-wideband surface plasmonic filter in microwave frequency," *Appl. Phys. Lett.*, vol. 104, no. 19, May 2014, Art. no. 191603.

[28] H. F. Ma, X. P. Shen, Q. Cheng, W. X. Jiang, and T. J. Cui, "Broadband and high-efficiency conversion from guided waves to spoof surface plasmonpolaritons," *Laser Photon. Rev.*, vol. 8, no. 1, pp. 146–151, 2014.

[29] B. C. Pan, Z. Liao, J. Zhao, and T. J. Cui, "Controlling rejections of spoof surface plasmonpolaritons using metamaterial particles," *Opt. Exp.*, vol. 22, no. 11, pp. 13940–13950, 2014.

[30] Z. Liao, J. Zhao, B. C. Pan, X. P. Shen, and T. J. Cui, "Broadband transition between microstrip line and conformal surface plasmon waveguide," *J. Phys. D, Appl. Phys.*, vol. 47, no. 31, 2014, Art. no. 315103.

[31] X. P. Shen and T. J. Cui, "Ultrathin plasmonic metamaterial for spoof localized surface plasmons," *Laser Photon. Rev.*, vol. 8, no. 1, pp. 137–145, 2014.

[32] Y. Yang, X. Shen, P. Zhao, H. C. Zhang, and T. J. Cui, "Trapping surface plasmonpolaritons on ultrathin corrugated metallic strips in microwave frequencies," *Opt. Exp.,* vol. 23, no. 6, pp. 7031–7037, 2015.